Facile abstraction of hydrogen atoms from graphane, diamond, and amorphous carbon surfaces: A first-principles study

Bhavin N. Jariwala,[1] Cristian V. Ciobanu,[2,*,†] and Sumit Agarwal[1,*,‡]
[1]*Department of Chemical Engineering, Colorado School of Mines, Golden, Colorado 80401, USA*
[2]*Division of Engineering, Colorado School of Mines, Golden, Colorado 80401, USA*
(Received 2 April 2010; revised manuscript received 8 June 2010; published 12 August 2010)

Abstraction of surface hydrogen by atomic H from graphane, diamond(001), diamond(111), and hydrogenated amorphous carbon (a-C:H) surfaces was studied using density-functional theory calculations in the generalized gradient approximation. Our calculations show that for each surface, the abstraction reaction is highly exothermic with a negligible activation energy barrier. The degree of exothermicity depends on the type of surface and on the local bonding environment of the site from which the H atom was abstracted. Detailed analyses of the reactions and of atomic charge densities along reaction pathways indicate a direct-impact Eley-Rideal mechanism for the abstractions.

DOI: 10.1103/PhysRevB.82.085418 PACS number(s): 82.65.+r

I. INTRODUCTION

The interaction of atomic H with group IV semiconductor surfaces such as Si, Ge, and C plays an important role in determining their growth mechanisms and electronic properties.[1–3] SiH_4,[2] GeH_4,[3] and a variety of hydrocarbon gases[1,4,5] are heavily diluted with H_2 during thermal and plasma-enhanced chemical-vapor deposition (PECVD) of nanocrystalline Si, Ge, and diamond, respectively. It has also been shown that the quality of epitaxial Si grown by PECVD improves with H_2 plasma exposure of the surface.[6] Room-temperature H_2 plasma exposure of amorphous Si prior to thermal crystallization reduces the crystallization time.[7] During epitaxial growth of Ge on Si(001), the interaction of atomic H with the growing Ge film suppresses island growth of Ge overlayers.[8] Although there are extensive reports on the interactions of hydrogen with Si, Ge, and C surfaces, the mechanism of atomic H interaction with carbon-based surfaces is relatively more complex than with Si or Ge due to the ability of carbon to form sp^3-, sp^2-, and *sp*-hybridization states.

The elementary reactions previously identified during H interaction with carbon surfaces are: H-abstraction, hydrogenation, and H-induced chemical etching.[9,10] Of these reactions, the abstraction of surface H atoms by atomic H is a critical step in determining the surface H coverage of graphane (H-terminated graphene), diamond, and a-C:H. Recently, the manipulation of the electronic properties of graphene sheets via H interaction to synthesize nanoscale graphane domains has generated a great deal of interest.[11–16] It was demonstrated that addition of H to graphene transforms the highly conductive sheet into an insulator.[11,14,17] A possible route for modifying the H coverage on graphane is the controlled abstraction of hydrogen. The abstraction of surface H is also a critical step for initiating growth in low-pressure PECVD of diamond from hydrocarbon gases heavily diluted in hydrogen.[4,18] Surface H abstraction creates active sites for subsequent chemisorption of hydrocarbon radicals leading to film growth.[19] During PECVD of a-C:H thin films from hydrocarbon plasmas, various interactions of atomic H with the surface (including abstraction) significantly affect the sp^3-to-sp^2 hybridization ratio and the H content in the film; this in turn determines the films' electronic and structural properties.[9] To our knowledge, no calculations have been performed to obtain the barrier for H abstraction by atomic H from graphane or a-C:H surfaces, although the reaction mechanism and the corresponding activation energy barrier have been widely speculated. Abstraction of H from a-C:H films by atomic H has been evidenced experimentally[20] based on isotope-exchange experiments and high-resolution electron-energy-loss spectroscopy by Lutterloh *et al.* These authors proposed an Eley-Rideal mechanism for abstraction from model a-C:H surfaces, in which the activation energy barrier was assumed to be small.

The activation energy barrier for atomic H abstraction has been primarily investigated for diamond surfaces. However, there is discrepancy in both the experimental and computational reports regarding the value of the energy barrier. The experimentally reported values for the barrier to H abstraction by atomic H from diamond surfaces range from ~0.29 to 0.69 eV.[21–24] A reason for the inconsistency in the experimental data could be that different procedures have been used to determine the barriers. For example, Krasnoperov *et al.*[22] fitted the experimental data to an Arrhenius expression using an experimental uncertainty in the rate constant and reported a barrier of 6.7 kcal/mol (0.29 eV). On the other hand, Koleske *et al.*[24] estimated the upper bound of the barrier to be 16 kcal/mol (0.69 eV) by assuming a 100% sticking probability for H addition and by evaluating the ratio of H addition to H abstraction. It should be noted that these values were obtained for polycrystalline diamond rather than for ideal (001) and (111) surfaces. The theoretically estimated values span a wide range as well,[25–32] from 0.0 (Ref. 30) to 0.93 eV.[31] All the theoretically reported activation energies are either obtained from model cluster calculations[25–27,29] or by using a hydrocarbon molecule as a model and imposing constraints on it so as to simulate a diamond (111) lattice.[28] No computational studies have been reported for the abstraction reaction on a-C:H surfaces, perhaps due to the difficulty in generating experimentally realistic surfaces. Using density-functional theory calculations based on the Perdew-Burke-Ernzerhof generalized gradient

 ©2010 The American Physical Society

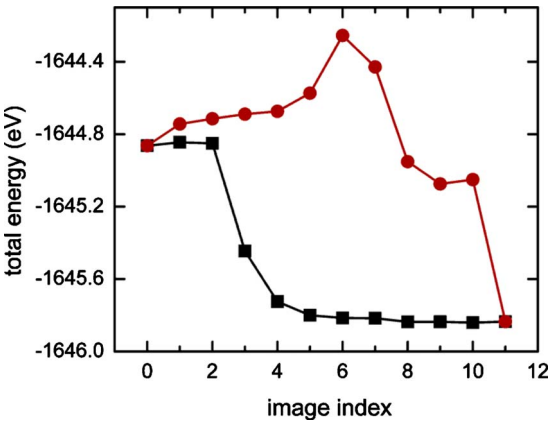

FIG. 1. (Color online) NEB transition state search with ten intermediate images for the abstraction of hydrogen from amorphous carbon. The energies of the image configurations on the starting (unoptimized) reaction path are shown as solid circles. The energies corresponding to the fully optimized pathway (shown as solid squares) decrease monotonically, indicating the lack of a reaction barrier for the abstraction from amorphous carbon.

approximation, we report the mechanism and the activation energy barrier for hydrogen abstraction by atomic H from graphane, diamond(001), diamond(111), and a-C:H surfaces. Compared to previous studies in the literature, we employ periodic supercells for simulation of surfaces, as opposed to model cluster calculations.[25–27,29] Graphane and diamond surfaces were computationally generated in a straightforward manner, as described herein. The a-C:H films were generated using a procedure based on molecular-dynamics simulations that involved tuning of the film density, H content, and the sp^2-to-sp^3 hybridization ratio of the carbon atoms.[10] Our calculations show that, for all carbon surfaces considered, the abstraction reaction proceeds via a highly exothermic, direct-impact Eley-Rideal mechanism with an insignificant activation energy barrier.

This paper is organized as follows. In Sec. II, we discuss the computational methodology employed to perform the *ab initio* calculations. We describe the specific results for the abstraction reactions on different surfaces in Sec. III and discuss these results in Sec. IV. In Sec. V, we summarize the key conclusions of this study and discuss implications on growth and modification of carbon-based surfaces.

II. COMPUTATIONAL METHODOLOGY

To investigate the abstraction of H from graphane, diamond, and a-C:H by an incoming hydrogen atom, we performed density-functional theory calculations using the Vienna *ab initio* simulation package (VASP).[33,34] Projector-augmented wave potentials[35] for carbon and hydrogen were used and calculations were performed in the generalized gradient approximation with the exchange-correlation functional of Perdew, Burke, and Ernzerhof.[36] Since hydrocarbon systems are typically not magnetic, the calculations were carried out in the absence of spin polarization. For calculations involving the graphane sheet and the diamond films, we used a vacuum spacing of 15 Å in the direction z normal to the film. For the a-C:H cluster calculations, the same vacuum spacing of 15 Å was used in all three directions. Based on single point energy calculations for bulk diamond structures performed for a range of lattice constants, we have determined a bulk diamond lattice constant of 3.572 Å, which agrees well with the experimental value of 3.56715 Å.[37] To study the abstraction from graphane, a 20.13 Å $\times$ 17.44 Å sheet containing 256 atoms (128 C and 128 H atoms) was created with periodic boundary conditions in the two in-plane directions (i.e., x and y). For abstraction from diamond, we employed a 7.58 Å $\times$ 7.58 Å diamond (001) film with 108 atoms (8 C layers and 2 H layers; 72 C and 36 H atoms) and a 10.1 Å $\times$ 8.75 Å diamond(111) film with 128 atoms (6 C layers and 2 H layers; 96 C and 32 H atoms). These films were also periodic in x and y directions, and the bottom two layers were passivated by H and fixed to simulate the underlying bulk. To study H abstraction from an a-C:H surface, we simulated a realistic film using the procedure described in an earlier work.[10] A cluster was carved out from this a-C:H film and the C atoms at the edge of the cluster were passivated with hydrogen. The abstraction of hydrogen from sp^3-hybridized and sp^2-hybridized C atoms was studied using this resulting cluster consisting of 250 atoms (144 C and 106 H). Since the cluster is relatively large and was created using a realistic a-C:H film, the interactions of an H atom with the cluster are comparable to its interactions with an a-C:H film. For all calculations, a plane-wave energy cutoff of 400 eV was employed and the Brillouin zone was sampled using the following Monkhorst-Pack k-point grids: $2\times2\times1$ for graphane, $5\times5\times1$ for the H:C(001) and H:C(111) surfaces, and $1\times1\times1$ for the clusters simulating amorphous carbon substrates.

In order to study the reaction pathways for the abstraction of hydrogen from the surface, we have set up nudged-elastic band (NEB) calculations.[38] In the NEB method, one starts with relaxed initial and final (postabstraction with an outgoing H_2 molecule) states, as well as with a number of intermediate configurations (images) which spatially connect the initial state with the final one. The NEB method evolves the system toward finding a saddle-point configuration given the initial and final states. For relaxing these two states, we have employed a conjugate-gradient algorithm which decreases the energy and optimizes the structure until the residual forces on any atom are smaller than 0.03 eV/Å. Interestingly, while relaxing the initial state, we noticed that the (incoming) H atom does not maintain its distance from the surface but proceeds toward it and abstracts the surface hydrogen. In other words, the initial states evolve into the final one through energy minimization toward a local minimum. For all the substrates simulated, we have found that abstraction of a surface H proceeds via conjugate-gradient relaxation as long as the initial distance of the incoming H atom with respect to the substrate is $\sim$2 Å; abstraction occurs during full relaxations of about $\sim$100–150 ionic steps.

The only possibility to relax an initial state without evolving it into the final one is to place the H atom farther away from the surface, e.g., at a height of $\sim$3 Å from the uppermost surface atom. The NEB calculates the energies of all the starting intermediate images and then proceeds to optimize these images to find a reaction pathway. In Fig. 1, we

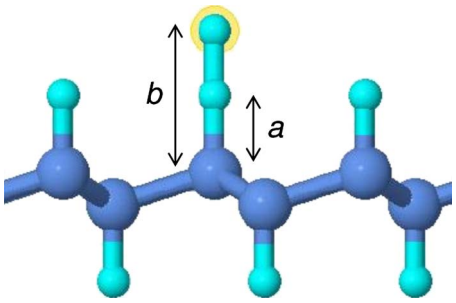

FIG. 2. (Color online) Supercell containing an incoming H atom and a graphane sheet. The distances a and b are used to define the reaction coordinate ε via Eq. (1).

show one of the more intensive NEB calculations that we performed for the abstraction of H from an sp^2 hybridized site of an amorphous substrate. We note that the system evolves from an unoptimized string of images (intermediate configurations) with a very large initial barrier, toward a fully optimized reaction pathway that shows monotonous decrease in the energy from one image to the next, i.e., zero-energy barrier. This is the same conclusion that we reached while relaxing the initial states using the conjugate-gradient relaxation. Needless to say, the NEB method and the conjugate-gradient relaxation are not equivalent and they serve different purposes. Still, in the rare cases in which reactions happen to be barrierless, they are both valid methods to reach such particular conclusion: the former because it is designed to search optimized reaction pathways and the latter because the evolution strictly downhill on the potential-energy surface takes the system into the reaction products. In what follows, we present only the results from relaxation.

III. RESULTS

For gas phase reactions such as $AB+C \rightarrow A+BC$, the rate of exchange of B depends on the motion of B as well as the motion of A relative to C.[39] Our choice of the reaction coordinate is thus based on the relative position of the incoming H, the surface H to be abstracted, and the carbon site from which H is abstracted. The reaction coordinate is defined as

$$\varepsilon = \frac{(a - a_{ini}) + |b - b_{ini}|}{(a_{fin} - a_{ini}) + (b_{fin} - b_{ini})}, \quad (1)$$

where a (b) is the distance between the surface hydrogen (incoming hydrogen) and the carbon site on the substrate (refer to Fig. 2). The subscripts *ini* and *fin* refer to the initial and the final values taken by the relevant distances.

We will first analyze the H abstraction from sp^3-hybridized C atoms on periodic surfaces of graphane, diamond(100), and diamond(111). We have also performed cluster calculations to study the H abstraction from sp^2- and sp^3-hybridized C atoms in a-C:H. As mentioned, the relaxations were started with the additional H atoms placed sufficiently far away from the substrates (2 Å) so that there is no significant interaction with the atoms of the surface. For all the abstraction reactions, the conjugate-gradient minimization of the total energy of the supercells resulted in the abstraction of surface hydrogen atoms, as shown in Figs. 3–5. We can therefore conclude that the facile H abstraction is due

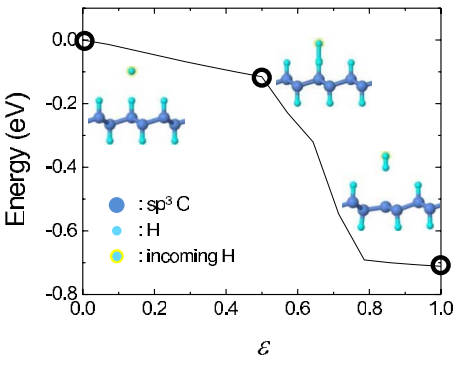

FIG. 3. (Color online) Energy of the supercell containing H and graphane as a function of the reaction coordinate ε. The reference energy (0.0 eV) is chosen for the initial configuration in which the H atom is sufficiently far from the surface. The circled data points on the curve and their respective images correspond to the initial, intermediate, and final states of the system. For clarity, the insets show only the (110) plane in which the abstraction reaction occurs.

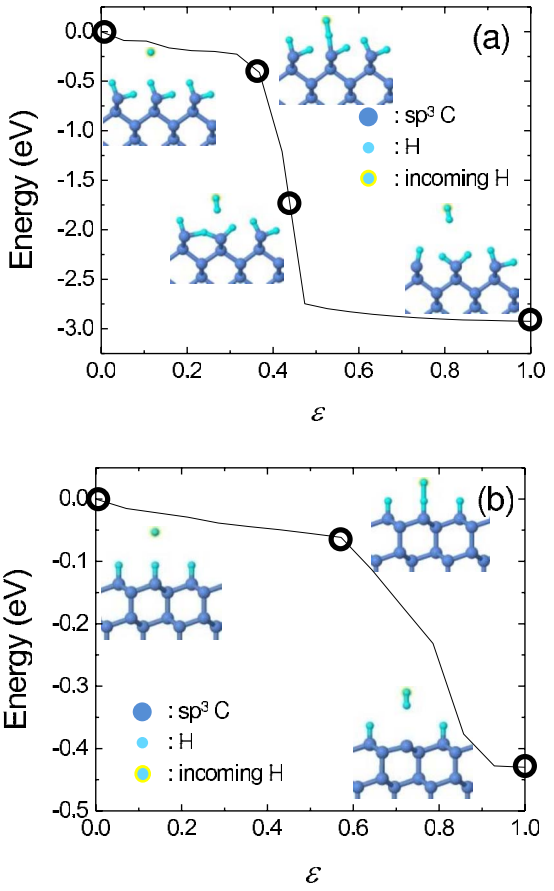

FIG. 4. (Color online) Energy of the supercells containing an incoming H atom and (a) an H:C(001) film, or (b) an H:C(111) film, as a function of the reaction coordinate. The circled data points on the curve and their respective images correspond to the initial, intermediate, and final states of the system. For clarity, the insets show only the (110) plane in which the abstraction reaction occurs.

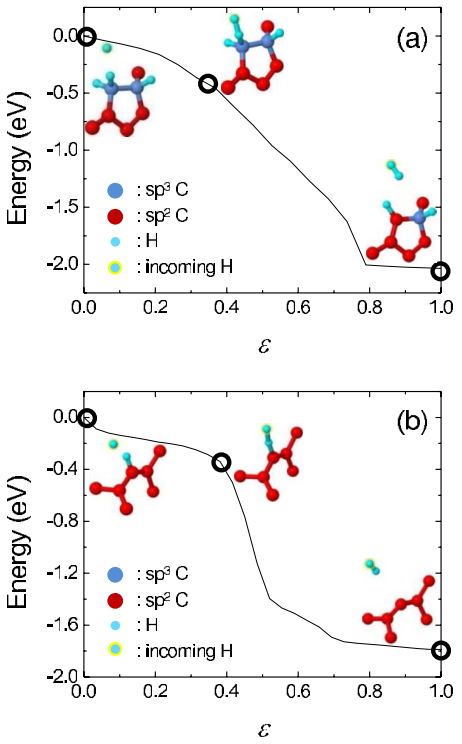

FIG. 5. (Color online) The abstraction reaction of H from (a) an sp^3-hybridized site and (b) sp^2-hybridized site in a 250-atom a-C:H cluster. For clarity, only the first few neighbors of the C atom that interacts with the incoming H atom are shown. The circled data points on the curve and their respective images correspond to the initial, intermediate, and final states of the system.

to a negligible activation energy barrier.[40] All abstraction reactions are exothermic with the exothermicities shown in Table I; the negative sign is kept to emphasize that the energy of the reaction products is smaller than that of the reactants.

The energetics of the H abstraction from a graphane sheet is shown in Fig. 3. The circled points on the energy curve and the images next to them show the initial, intermediate, and final states of the supercell. After abstraction, the C atom had three C neighbors and a dangling bond was created: in order to minimize its energy, the C atom converts to a more sp^2-like configuration as compared to the tetrahedral configuration of the sp^3 C atoms in graphane. Figures 4(a) and 4(b) show H abstraction from unreconstructed H:C(001) and unreconstructed H:C(111) films, respectively. In the case of the dihydride H:C(001) surface, the H atoms on each carbon site are not symmetric, but are canted in order to relieve the steric repulsion which is present in case of symmetric dihydrides.[41] After abstraction, an H atom from a nearby C site transfers to the abstraction site [refer to Fig. 4(a)]. For the H:C(111) film, a dangling bond was created on the C atom from which the H atom was abstracted. After the creation of the dangling bond, the C atom lowered its energy by assuming a relatively more planar configuration, similar to that of the C abstraction site in graphane.

TABLE I. Summary of various abstraction reactions for different C-based substrates. The exothermicities for the sp^3 and sp^2 C sites in a-C:H depend on the local bonding environment of the specific C site from which H is abstracted; as such, they may differ from site to site on the same film or from one a-C:H film to another.

Substrate	Barrier (eV)	Exothermic reaction energy (eV)
Graphane sheet	Negligible	−0.71
H:C(100) film	Negligible	−2.92
H:C(111) film	Negligible	−0.45
a-C:H (sp^3 C)	Negligible	−2.03
a-C:H (sp^2 C)	Negligible	−1.79

Figure 5(a) shows the energetic reaction progress for H abstraction from a sp^3-hybridized C atom in an a-C:H cluster. For clarity only the first few neighboring atoms of the atom that interacts with the incoming H are shown. After the H abstraction, the C atom from which the H atom was abstracted changed its hybridization from sp^3 to sp^2 to avoid the formation of a dangling bond. For understanding H abstraction from an sp^2-hybridized C atom in a-C:H, an H atom was placed 2 Å away from an sp^2-hybridized C atom in the 250-atom a-C:H cluster. Abstraction as well as hydrogenation reactions were observed at different sp^2 C sites in the cluster, and both of these reactions were barrierless.[10] Figure 5(b) shows the energetic progress for the abstraction of H from an sp^2 C atom in a-C:H by an incoming H atom. In the case of abstraction from an sp^2-hybridized C atom in a-C:H, a dangling bond was created on the sp^2-hybridized C site.

IV. DISCUSSION

The visualization of various intermediate states for each of the reactions indicates an Eley-Rideal mechanism[42,43] for abstraction. As opposed to the Langmuir-Hinshelwood mechanism, where the incoming species adsorbs and stays on the surface prior to reaction, in the Eley-Rideal mechanism the incoming species directly reacts with the surface species upon impact:[44] the incoming H atom approaches the surface and reacts with the surface H atom to form an H_2 molecule, which desorbs. To illustrate the Eley-Rideal mechanism further and to explain the physical origin of the barrierless abstraction process, we have considered the example of H abstraction from graphane. We have plotted the electron densities (Fig. 6) for the supercell at different reaction coordinates during the relaxation process. From Fig. 6(a) we can see that initially the charge density of the incoming H does not overlap with the charge density of the H atom on graphane. The incoming H atom consists of a single-electron bound to the nucleus. In its ground state, the electron in the incoming H atom is in the 1s state and the charge density, i.e., the probability density for locating the electron, is spherical. As the H atom approaches the graphane sheet, the charge density of the incoming H overlaps with that of the H atom on graphane [Figs. 6(b) and 6(c)]. The C-H bond of graphane becomes weaker as indicated by the decrease in the charge density between the respective C and H atoms. At the same time, as seen in Figs. 6(b) and 6(c), the interaction between the incoming H atom and the H atom on the surface

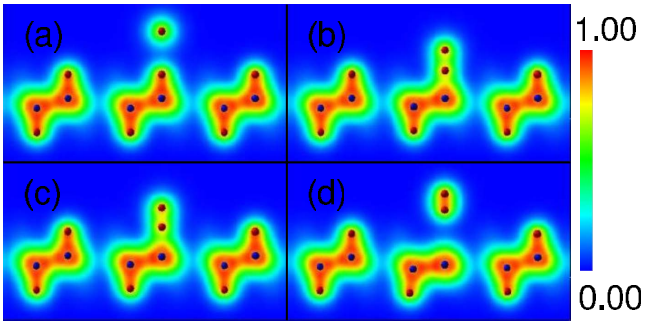

FIG. 6. (Color online) Cross-sectional view of the charge densities of the atoms in the supercell containing H and graphane at various points along the reaction pathway. Panel (a) corresponds to the initial state, (b) and (c) correspond to intermediate states, and (d) to the final state. The color scale on the right indicates the electron density in arbitrary units.

increases as shown by a gradual increase in the charge density in between these two H atoms. Finally, in Fig. 6(d) we observe that the C-H bond is broken and the H on the surface is abstracted via formation of an H_2 molecule. Similar observations hold for the other substrates we use. Hence, we conclude that the physical origin for facile abstraction observed during the relaxation is the preference of the surface H to share its electron with the highly reactive incoming H, rather than to passivate the surface C atom.

The considerable difference in the values of the energy released during the H abstraction from the different substrates (see Table I) can be explained based on the local bonding environment of the C atom on the surface after abstraction. For each of the periodic substrates, diamond (001), diamond (111), and graphane, the H abstraction occurs at an sp^3 C site. The reason for the substantial difference in the energy released from diamond (001) as compared to diamond (111) is the more pronounced structural relaxation that takes place in the case of the dihydride surface. The incoming H atom abstracts the topmost H from the surface C site which is thus left reactive; as such, this reactive surface site takes an H from a nearby carbon site forming a new dihydride at the adsorption site [refer to the insets in Fig. 4(a)]. The dihydride just formed has now sufficient room to arrange itself symmetrically, given that the nearby C only has one H atom which points perpendicular to the surface. On the other hand, after abstraction the C atom on diamond(111) is left with a dangling bond and little room to relax [Fig. 4(b)]. Therefore, postabstraction, the C atom on diamond(001) has a much more stable configuration than the C atom on diamond(111) which explains the large difference in exothermicity for the two reactions.

The surface of graphane consists of monohydride C atoms similar to the surface of diamond(111). In both cases, after abstraction the C atom has a dangling bond and assumes a relatively more planar configuration. This is because the C atom with the dangling bond tries to minimize its energy by allowing shorter C-C bond lengths with the neighboring C atoms so that it can convert to a more planar geometry without perturbing the surrounding lattice. The relatively small difference in the energy released after H abstraction from diamond (111) and graphane is due to the extent of planarity that the C atom can assume after abstraction. In diamond (111) the C-C bond length between the C that loses the H atom and its neighbors decreases from 1.54 to 1.49 Å after abstraction. For graphane, the equivalent C-C bond length changes from 1.52 to 1.48 Å. The C-C-C bond angle on the surface from where H is abstracted changes from 110.4° to 114.2° for diamond(111) and it changes from 111.3° to 117.8° for graphane. Thus, graphane can accommodate the dangling bond on the C atom on its surface in a relatively more stable manner and minimize its energy by assuming a more planar configuration than the C atom on diamond(111). Therefore, the energy released after the H abstraction from graphane is larger than that released upon abstraction from diamond(111).

The abstraction from an sp^3 C site in a-C:H film is more exothermic than abstraction from a sp^2 C site (see Table I). After abstraction, the sp^3 C site changes its hybridization to sp^2 and avoids the formation of a dangling bond [Fig. 5(a)]. The change in hybridization is evidenced by alteration in the bond angles and bond lengths of the C atom with its neighbors after abstraction. Before abstraction, the sp^3 C has four nearest neighbors (2 C and 2 H) with a tetrahedral geometry. The C-C bond length between the C atom from which H is abstracted and its sp^2 C neighbor [dark (red online) neighboring C atom in Fig. 5] is 1.5 Å. After abstraction, the same C atom has three neighbors (2 C and 1 H) with a planar geometry and the C-C bond length with its sp^2 C neighbor changes to 1.37 Å. Therefore, postabstraction, the C atom avoids the formation of a dangling bond by changing its hybridization to sp^2 and forming a stronger bond with its sp^2 C neighbor. In the case of abstraction from a sp^2 C site, the C atom that loses the H atom has a dangling bond after abstraction [Fig. 5(b)]. Prior to abstraction the sp^2 C has three neighbors (2 C and 1 H). After abstraction the C atom is left with only two nearest neighbors. Since both the remaining neighbors are sp^2 C atoms, the C atom cannot change its hybridization and a dangling bond remains on the atom. Thus, postabstraction the sp^3 C site does not have a dangling bond making it relatively more stable than the sp^2 C site with a dangling bond. Hence, abstraction from the sp^3 C site is more exothermic than abstraction from the sp^2 C site in a-C:H.

V. SUMMARY AND CONCLUSIONS

The H-abstraction reactions from graphane, diamond(001), diamond(111), and a-C:H surfaces by atomic H were investigated using *ab initio* calculations. We have shown that the abstraction reactions from various surfaces are highly exothermic with a negligible barrier. Abstraction occurs via a direct-impact Eley-Rideal mechanism, similar to other semiconductor surface such as those of silicon.[42,43] Similar to Si, the abstraction reaction plays an important role in determining the surface H coverage and the growth mechanism of carbon-based materials. For example, barrierless H abstraction from graphane could have potential implications in developing strategies to tailor its band gap. Recent experiments have demonstrated that longer H_2 plasma expo-

sures at a higher plasma power are required to completely hydrogenate one layer of graphene as opposed to two or three layers.[12] The reason for higher plasma power and exposure time was attributed to the relatively high hydrogenation barrier for a single graphene layer compared to two or three layers.[12] We speculate that an added reason for the slower hydrogenation rate for one layer of graphene could be the simultaneous H abstraction from the single layer: the rate of hydrogenation would then compete with the rate of abstraction to obtain complete coverage of hydrogen on graphene to form graphane. Currently, the hydrogen coverage on graphene is modified via dehydrogenation by heating partially hydrogenated graphene or graphane.[12] An alternative to tailor the band gap of graphene could be controlled barrierless H abstraction from graphane to modify the surface coverage of hydrogen at lower temperatures.

The barrierless Eley-Rideal mechanism for H abstraction from diamond and a-C:H provides an important insight in the possible mechanism of growth of diamond, diamondlike carbon, and a-C:H using PECVD of hydrocarbon gases that are heavily diluted in hydrogen. The dangling bonds created after the barrierless abstraction, as shown in Figs. 4(b) and 5(b), could aid film growth by providing chemisorption sites for the hydrocarbon radicals.[1,9]

ACKNOWLEDGMENTS

This research was supported by the ACS-PRF (Grant No. 44934-G5), the NSF under Grants No. CMMI-0825592 and No. CBET-0846923, and the Renewable Energy MRSEC program at the Colorado School of Mines (NSF under Grant No. DMR-0820518). We also acknowledge the use of supercomputing resources provided by the Golden Energy Computing Organization at CSM.

*Corresponding author.
†cciobanu@mines.edu
‡sagarwal@mines.edu

[1] J. C. Angus and C. C. Hayman, Science **241**, 913 (1988).
[2] S. Sriraman, S. Agarwal, E. S. Aydil, and D. Maroudas, Nature (London) **418**, 62 (2002).
[3] P. R. Poulsen, M. Wang, J. Xu, W. Li, K. Chen, G. Wang, and D. Feng, J. Appl. Phys. **84**, 3386 (1998).
[4] J. C. Angus, H. A. Will, and W. S. Stanko, J. Appl. Phys. **39**, 2915 (1968).
[5] B. Y. Hong, M. Wakagi, W. Drawl, R. Messier, and R. W. Collins, Phys. Rev. Lett. **75**, 1122 (1995).
[6] W. G. Townsend and M. E. Uddin, Solid-State Electron. **16**, 39 (1973).
[7] K. Pangal, J. C. Sturm, S. Wagner, and T. H. Buyuklimanli, J. Appl. Phys. **85**, 1900 (1999).
[8] D. Dentel, J. L. Bischoff, T. Angot, and L. Kubler, Surf. Sci. **402-404**, 211 (1998).
[9] J. Kuppers, Surf. Sci. Rep. **22**, 249 (1995).
[10] B. N. Jariwala, C. V. Ciobanu, and S. Agarwal, J. Appl. Phys. **106**, 073305 (2009).
[11] D. C. Elias, R. R. Nair, T. M. G. Mohiuddin, S. V. Morozov, P. Blake, M. P. Halsall, A. C. Ferrari, D. W. Boukhvalov, M. I. Katsnelson, A. K. Geim, and K. S. Novoselov, Science **323**, 610 (2009).
[12] Z. Luo, T. Yu, K.-j. Kim, Z. Ni, Y. You, S. Lim, Z. Shen, S. Wang, and J. Lin, ACS Nano **3**, 1781 (2009).
[13] B. S. Pujari and D. G. Kanhere, J. Phys. Chem. C **113**, 21063 (2009).
[14] J. O. Sofo, A. S. Chaudhari, and G. D. Barber, Phys. Rev. B **75**, 153401 (2007).
[15] H. J. Xiang, E. J. Kan, S. H. Wei, M. H. Whangbo, and J. L. Yang, Nano Lett. **9**, 4025 (2009).
[16] A. K. Singh and B. I. Yakobson, Nano Lett. **9**, 1540 (2009).
[17] S. Lebègue, M. Klintenberg, O. Eriksson, and M. I. Katsnelson, Phys. Rev. B **79**, 245117 (2009).
[18] S. Matsumoto, Y. Sato, M. Tsutsumi, and N. Setaka, J. Mater. Sci. **17**, 3106 (1982).
[19] M. Frenklach, J. Appl. Phys. **65**, 5142 (1989).
[20] C. Lutterloh, A. Schenk, J. Biener, B. Winter, and J. Kuppers, Surf. Sci. **316**, L1039 (1994).
[21] S. J. Harris and A. M. Weiner, J. Appl. Phys. **74**, 1022 (1993).
[22] L. N. Krasnoperov, I. J. Kalinovski, H. N. Chu, and D. Gutman, J. Phys. Chem. **97**, 11787 (1993).
[23] B. D. Thoms, J. N. Russell, P. E. Pehrsson, and J. E. Butler, J. Chem. Phys. **100**, 8425 (1994).
[24] D. D. Koleske, S. M. Gates, B. D. Thoms, J. N. Russell, and J. E. Butler, J. Chem. Phys. **102**, 992 (1995).
[25] S. Skokov and J. M. Bowman, J. Chem. Phys. **113**, 779 (2000).
[26] R. C. Brown, C. J. Cramer, and J. T. Roberts, J. Phys. Chem. B **101**, 9574 (1997).
[27] H. F. Lu and Y. C. Sun, Diamond Relat. Mater. **11**, 1560 (2002).
[28] M. Page and D. W. Brenner, J. Am. Chem. Soc. **113**, 3270 (1991).
[29] X. Y. Chang, M. Perry, J. Peploski, D. L. Thompson, and L. M. Raff, J. Chem. Phys. **99**, 4748 (1993).
[30] S. M. Valone, M. Trkula, and J. R. Laia, J. Mater. Res. **5**, 2296 (1990).
[31] X. M. Song, M. Wang, B. Wang, G. H. Chen, and H. Yan, Thin Solid Films **395**, 257 (2001).
[32] C. Kanai, K. Watanabe, and Y. Takakuwa, Appl. Surf. Sci. **159-160**, 599 (2000).
[33] G. Kresse and J. Furthmuller, Phys. Rev. B **54**, 11169 (1996).
[34] G. Kresse and J. Furthmuller, Comput. Mater. Sci. **6**, 15 (1996).
[35] G. Kresse and D. Joubert, Phys. Rev. B **59**, 1758 (1999).
[36] J. P. Perdew, K. Burke, and M. Ernzerhof, Phys. Rev. Lett. **77**, 3865 (1996).
[37] H. Holloway, K. C. Hass, M. A. Tamor, T. R. Anthony, and W. F. Banholzer, Phys. Rev. B **44**, 7123 (1991).
[38] G. Henkelman and H. Jonsson, J. Chem. Phys. **113**, 9978 (2000).
[39] K. Sumathi and A. K. Chandra, J. Photochem. Photobiol., A **43**, 313 (1988).
[40] E. Machado, M. Kaczmarski, P. Ordejón, D. Garg, J. Norman,

and H. Cheng, Langmuir **21**, 7608 (2005).
[41] Y. Yu, C. Z. Gu, L. F. Xu, and S. B. Zhang, Phys. Rev. B **70**, 125423 (2004).
[42] S. Agarwal, S. Sriraman, A. Takano, M. C. M. van de Sanden, E. S. Aydil, and D. Maroudas, Surf. Sci. **515**, L469 (2002).
[43] S. Agarwal, A. Takano, M. C. M. d. Sanden, D. Maroudas, and E. S. Aydil, J. Chem. Phys. **117**, 10805 (2002).
[44] W. H. Weinberg, in *Advances in Gas-Phase Photochemistry and Kinetics*, edited by M. N. R. Ashfold and C. T. Rettner (The Royal Society of Chemistry, Letchworth, 1991), pp. 171–219.